Electronic Supplementary Material (ESI) for Soft Matter.
This journal is © The Royal Society of Chemistry 2014

Supplementary Information

Colloidal Structures of Asymmetric Dimers via Orientation-dependent Interactions

Fuduo Ma,[1] Sijia Wang,[1] Hui Zhao,[2] David T. Wu,[3] and Ning Wu[1,*]

[1]Department of Chemical and Biological Engineering, Colorado School of Mines, Golden, Colorado 80401

[2]Department of Mechanical Engineering, University of Nevada, Las Vegas, Nevada 89154

[3]Department of Chemistry and Geochemistry, Colorado School of Mines, Golden, Colorado 80401

1. Supplementary figures

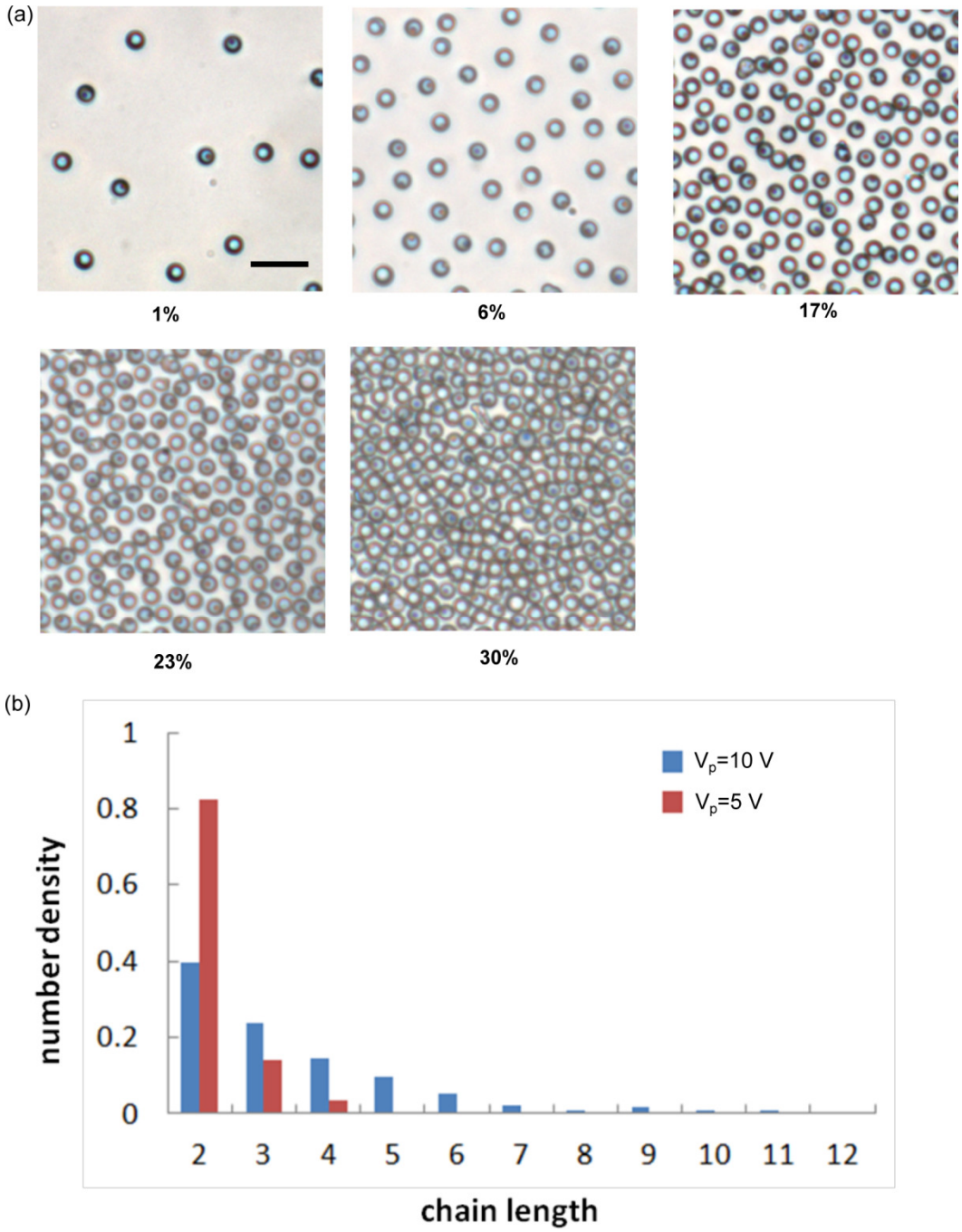

Figure S1 (a) Optical images of the standing asymmetric dimers at different particle densities (V_p =5 V and ω=6.5 kHz). Scale bar: 10μm. (b) The distribution of linear chain lengths at different voltages.

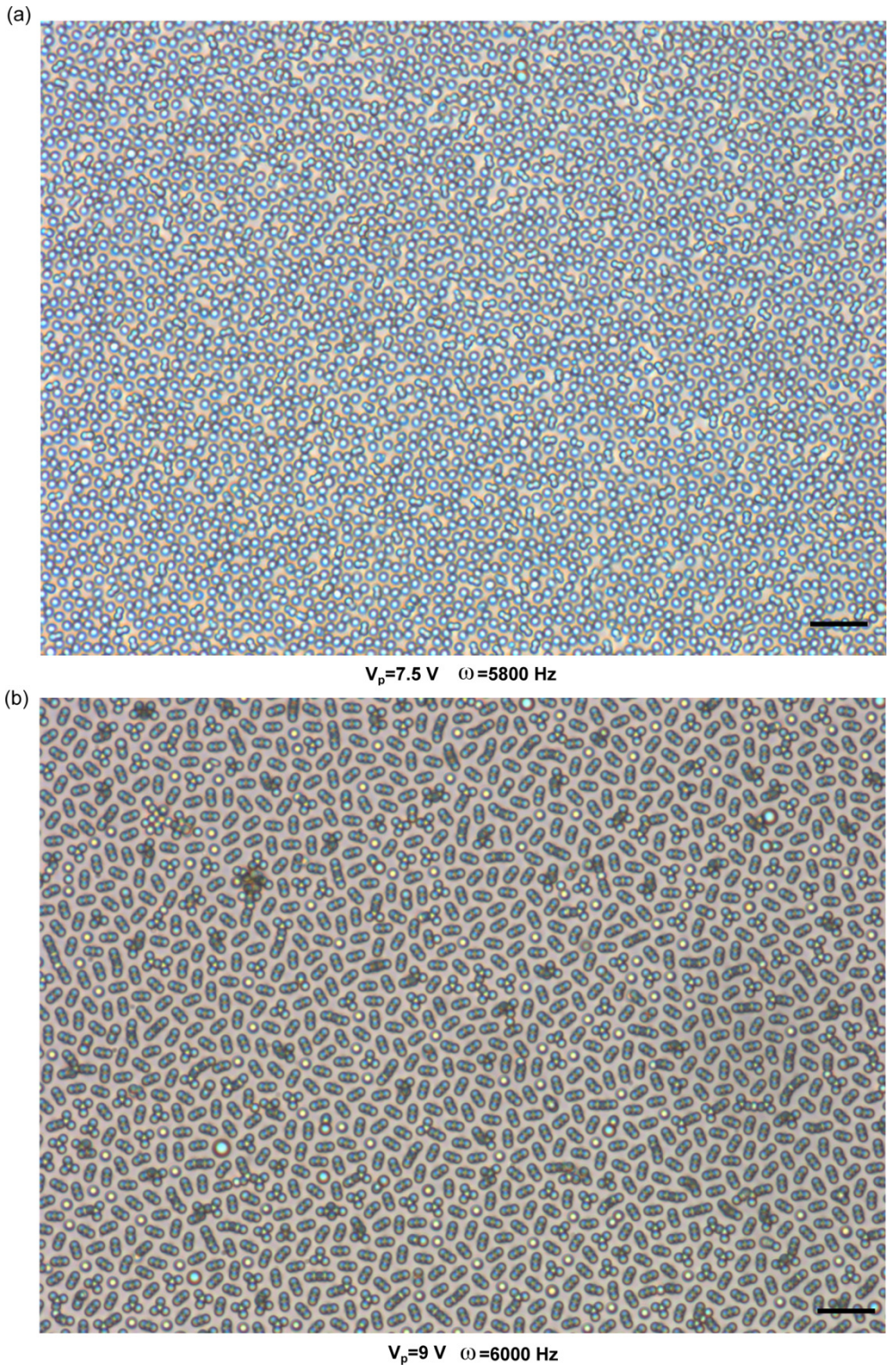

Figure S2 (a) Symmetric dimers ($R_1 = 0.84\,\mu m$ and $R_2 = 0.74\,\mu m$) show no sign of aggregation. (b) Spherical particles ($R = 1\ \mu m$) assemble into zig-zag trimers and chains. Scale bar: 20 μm.

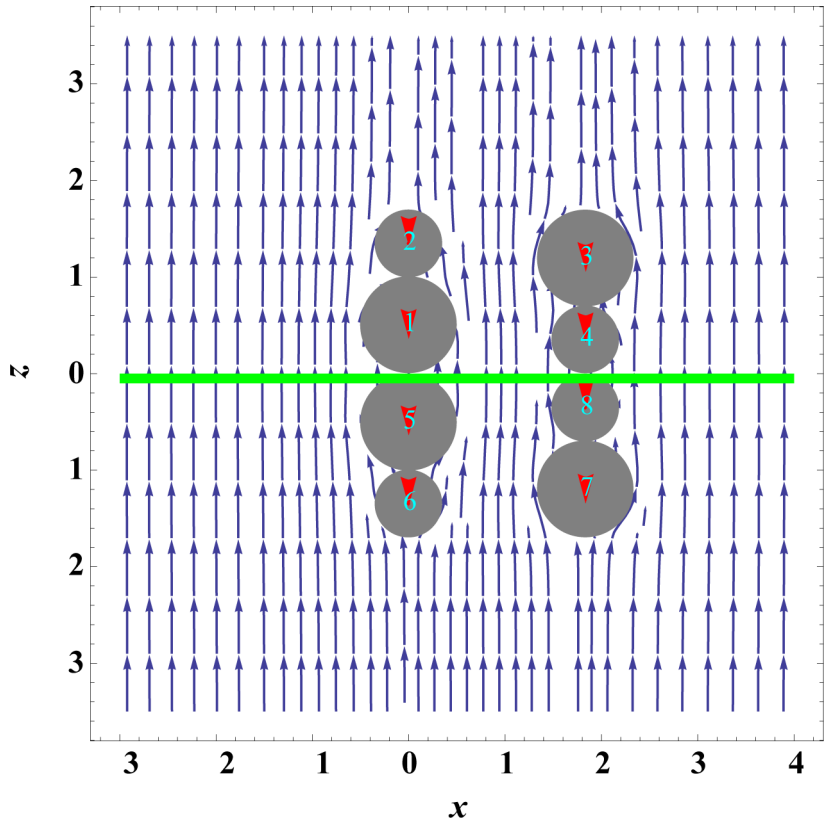

Figure S3 A typical calculation of the induced dipoles and their local electric fields between a pair of standing dimers. The field lines are illustrated in blue. The red arrows show the dipole directions. The green illustrates the substrate. Spheres 5-8 represent image charges and dipoles. The external electric field is aligned with the z-direction. Parameters used in the calculations correspond to typical experiment conditions: $R_1 = 1.27\,\mu\text{m}$, $R_2 = 0.89\,\mu\text{m}$, $\zeta_1 = \zeta_2 = -60\,\text{mV}$, $\varepsilon = 78$ (for water), $V_p = 8\,\text{V}$, $2H = 100\,\mu\text{m}$, $\omega =$ 6.5 kHz, and $\kappa^{-1} \sim 150\,\text{nm}$.

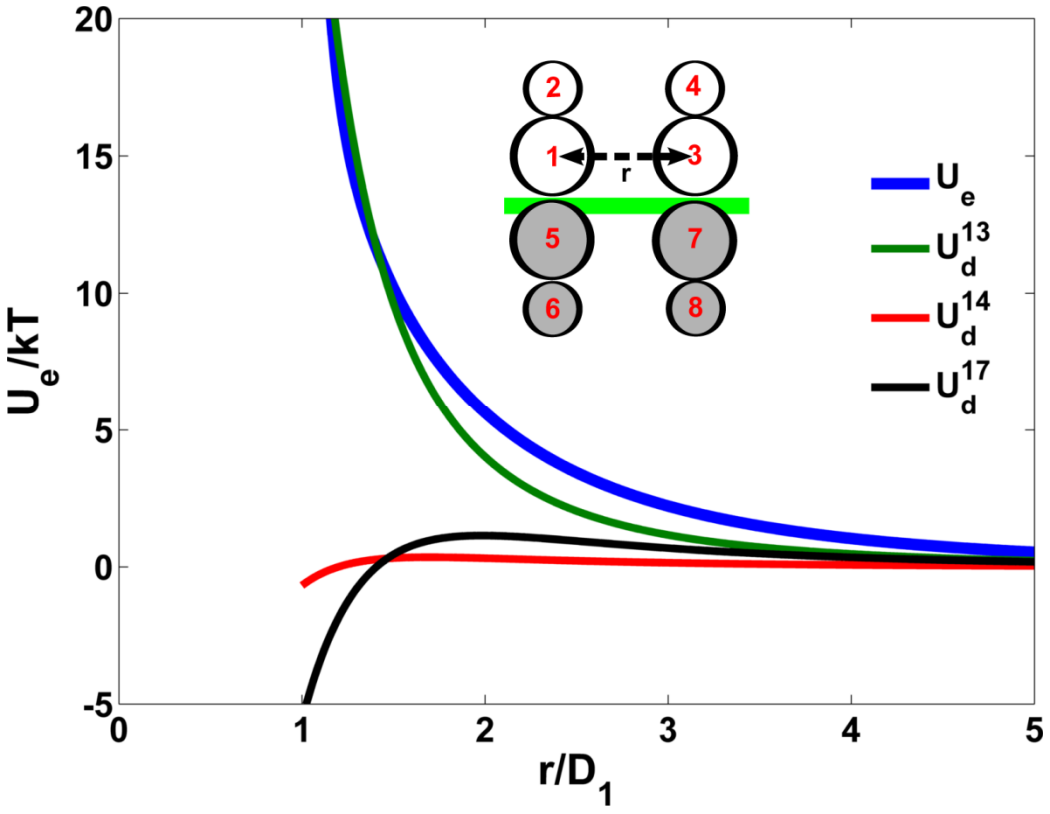

Figure S4 The electrostatic pair interaction U_e (scaled by the thermal energy) between "up-up" dimers and breakdown of the contribution from dipolar interactions U_d^{ij} between different lobes. The particle separation is scaled by the large lobe diameter. See text for calculation details. Inset: the system of dimers is approximated by individual spheres. The substrate is illustrated in green and grey spheres are (charge and dipole) images.

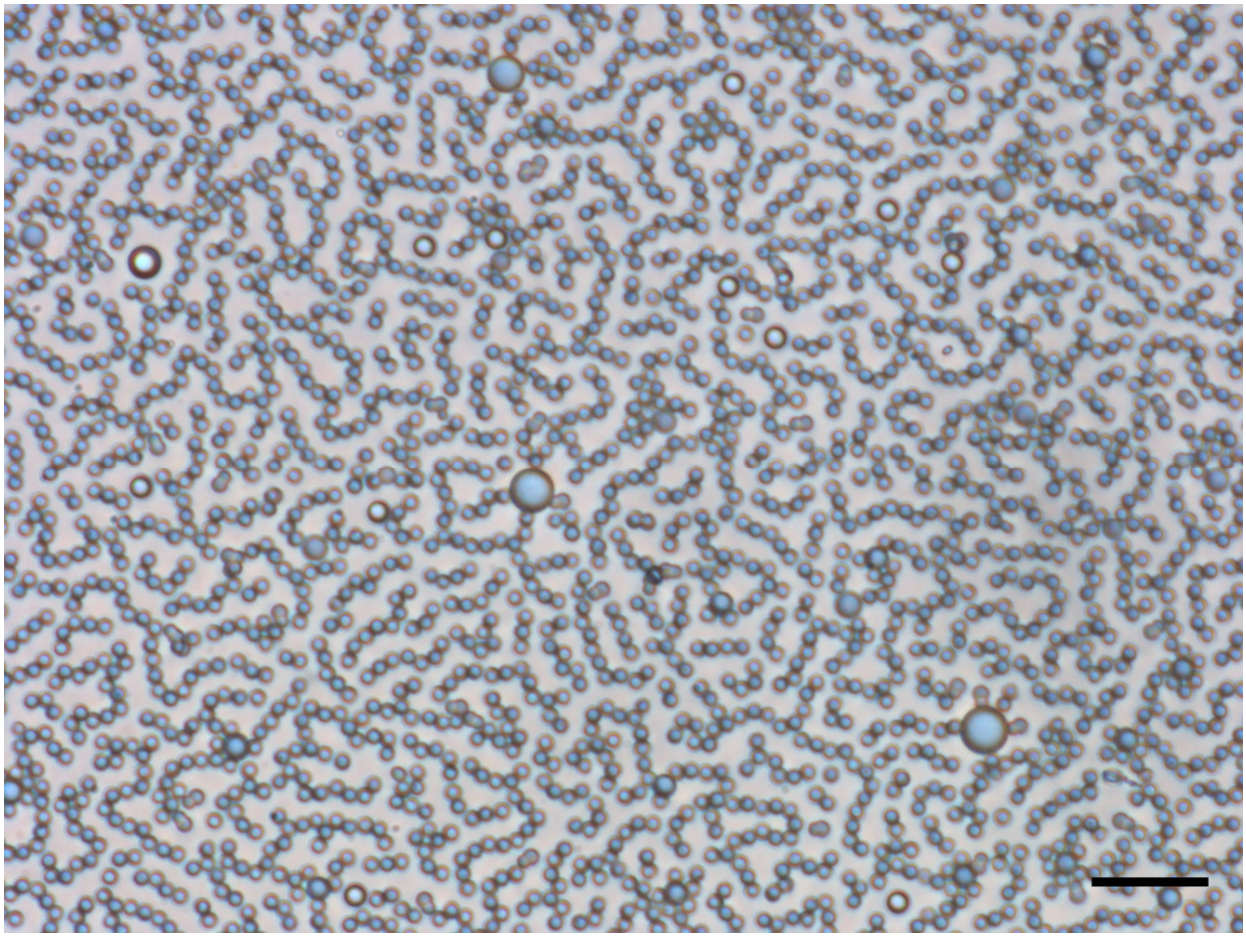

Figure S5 Well-separated linear chains (formed by alternating "up" and "down" dimers) at intermediate densities. Scale bar: 20μm. The applied voltage field is V_p=8 V and ω=4.4 kHz.

2. The electrohydrodynamic (EHD) interaction between dimers

The EHD interaction can be calculated based on the following method. Assuming that we know the EHD velocity $u_{EHD}(r)$, we can calculate the drag force by using the Stoke's law, i.e., $F(r)=6\pi\mu u_{EHD}(r)R$. The effective EHD interaction potential will be obtained by integrating this force over the separation between particles, i.e., $\phi_{EHD}(r)=\int_{r}^{\infty}F(r')dr'$. This method has been previously utilized to calculate the drag force and EHD interactions between spherical particles by several groups.[1, 2] The key is to obtain the EHD velocity $u_{EHD}(r)$ for both "up" and "down" dimers. Here we will first derive the $u_{EHD}(r)$ for spherical particles. We will then extend our derivation to dimers.

2.1 The EHD velocity for a spherical particle

Ristenpart and his colleagues have derived the scaling law for the EHD velocity of a spherical particle,[3, 4] which is the foundation of our derivation. However, we recently identified an inconsistency in their formula. Here we will summarize our results, which reveal a subtle difference from what has been reported before.

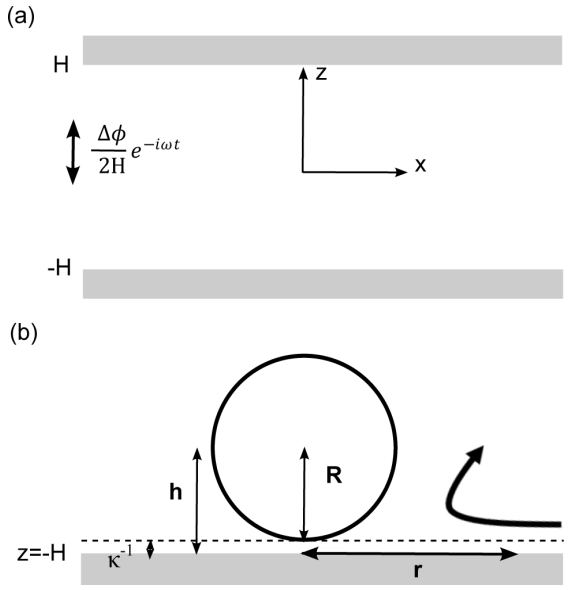

Fig. S6 Schematic illustrating important geometric parameters for the calculation of EHD interactions. Two electrodes are separated by $2H \sim 100\ \mu m$. The applied AC voltage is represented by $V_p e^{-j\omega t}$. The sphere is located near the substrate, where its distance from the substrate $h \sim R$, assuming that the Debye length κ^{-1} is much smaller than the radius R. When $u_{EHD}(r)$ is negative, the solvent is directed towards the particle (shown by the arrow). Otherwise, the flow is directed away from the particle.

All relevant geometric parameters are shown schematically in Fig. S6. We start from the potential distribution between two electrodes when they are subject to an externally applied AC bias $V_p e^{-j\omega t}$, i.e., Eq. (2.6)[4] or equivalently Eq. (21)[5] in Ref. 4 and 5, respectively. For frequencies $\omega \ll \kappa^2 D$ (where ω is the frequency, κ^{-1} is the Debye length, and D is the diffusion coefficient of the ions), one can show that the applied electric field within the diffusive layer of the electrode is

$$E_0\left(z \sim -H\right) \sim \frac{V_p}{2H} e^{-j\omega t} \frac{\left(\kappa H + \alpha^2\right) + j\alpha\left(\kappa H - 1\right)}{1+\alpha^2} \tag{S1}$$

where V_p is the peak voltage applied between electrodes, and $\alpha = \omega H / \kappa D$. Depending on the frequency, salt concentration, and electrode separation, α can be larger, comparable, or less than one. The applied electric field far away from the diffusive layer is

$$E_0\left(|z| \ll H\right) \sim \frac{V_p}{2H} e^{-j\omega t} \frac{\alpha^2 - j\alpha}{1+\alpha^2} \tag{S2}$$

Therefore, the amount of induced charge within the diffusive layer can be obtained as

$$\begin{aligned} q &= \int_{-H}^{0} \rho dz = \varepsilon\varepsilon_0 \left[E_\infty\left(|z| \ll H\right) - E_\infty(z \sim -H) \right] \\ &= -\varepsilon\varepsilon_0 \frac{V_p}{2H} e^{-j\omega t} \frac{\kappa H\left(1 + j\alpha\right)}{1+\alpha^2} \end{aligned} \tag{S3}$$

We note that Eq. (S3) is different from Eq. (2.13) in Ref. 4,[4] where a non-zero term in the electric field far away from the diffusive layer was missing. More importantly, our expression

gives the expected high frequency limit, i.e., when $\omega \to \infty$ ($\alpha \to \infty$), the induced charges within the diffusive layer diminish.

In order to induce an EHD flow, a tangential electric field needs to act on the induced charges. This tangential field arises from the tangential component of the electric field generated by the induced dipole of a sphere. It can be expressed as[3, 6]

$$E_t \sim E_{dipole} \cdot \hat{x} \sim -\frac{p_{dipole}}{4\pi\varepsilon\varepsilon_0} \frac{3Rr}{\left(R^2 + r^2\right)^{5/2}} \tag{S4}$$

where $\hat{x}$ is a unit vector in the x direction, p_{dipole} is the induced dipole moment of the sphere, and r is the distance from the particle center line to the point where the EHD flow is evaluated.[3] In Eq. (S4), we have assumed that the separation between the particle and the substrate h can be approximated by the radius R, given that $\kappa^{-1} \ll R$. The induced dipole moment can be further expressed as[6]

$$p_{dipole} = 4\pi\varepsilon\varepsilon_0 R^3 E_0 K \tag{S5}$$

where $K = K' + jK''$ is the complex Clausius-Mossotti factor[6] or the polarization coefficient.[7] Both the real (K') and imaginary part (K'') of K sensitively depend on a variety of process parameters[7] including ω, R, D, κ^{-1}, and zeta potential ζ. Substituting Eq. (S2) and Eq. (S5) into Eq. (S4), one can obtain the expression for the tangential electric field

$$E_t \sim -\frac{V_p}{2H} e^{-j\omega t} \frac{\alpha^2 - j\alpha}{1+\alpha^2} \left(K' + jK''\right) \frac{3\left(r/R\right)}{\left[1+\left(r/R\right)^2\right]^{5/2}} \tag{S6}$$

The EHD velocity can then be calculated

$$u_{EHD} \sim \frac{\left\langle q \cdot E_t \right\rangle}{\mu\kappa} = \frac{\mathrm{Re}\left(q \cdot E_t^*\right)}{2\mu\kappa} = \frac{CK''}{\mu} \frac{3\left(r/R\right)}{2\left[1+\left(r/R\right)^2\right]^{5/2}} \tag{S7}$$

where $C = \varepsilon\varepsilon_0 \left(\frac{V_p}{2H} \right)^2 \frac{\alpha^2}{1+\alpha^2} \frac{\kappa D}{\omega}$. Note that Eq. (S7) is surprisingly simple. The EHD velocity is proportional to the square of the applied field $V_p / 2H$, a signature of the nonlinear electrokinetics. More importantly, our results indicate that the sign of the EHD flow (i.e., the direction of the flow), is uniquely determined by the sign of the imaginary part of the polarizability coefficient K''. When K'' is negative, the solvent is directed towards the particle, which could potentially cause the aggregation of neighboring particles. When K'' is positive, the flow will be directed away from the particle. This result is different from the expression in Ref. 4, where both real (K') and imaginary (K'') parts of the polarization coefficient are important[4] in u_{EHD}. A rigorous test of this new prediction is beyond the scope of this paper, but will be published elsewhere.

2.2 The EHD velocity for standing dimers

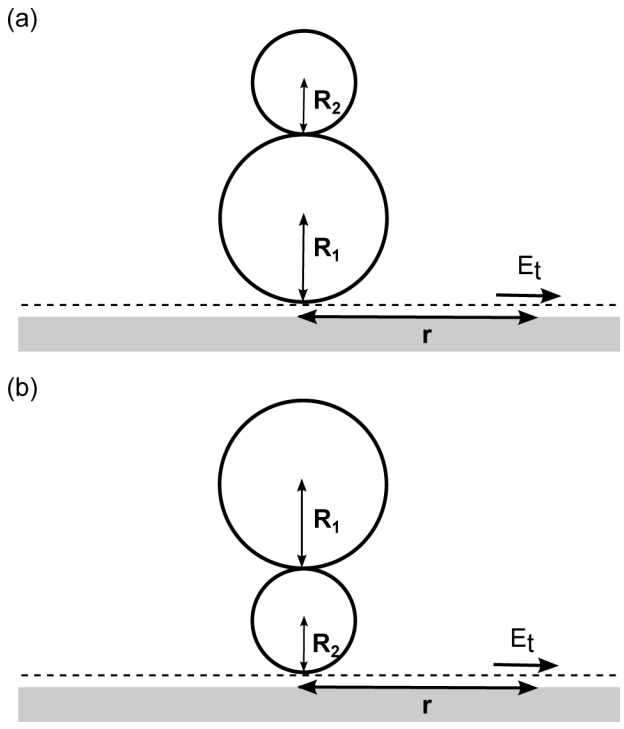

Fig. S7 The tangential electric field generated by the induced dipole of a dimer has contributions from both top and bottom lobes.

Now we extend the above derivation to a standing dimer, either in the "up" or "down" orientation. The only difference from the spherical particle is that the tangential electric field E_t now consists of the dipolar field generated by both bottom and top lobes, i.e., $E_t(r)=\left[E_{dipole,1}(r)+E_{dipole,2}(r)\right]\cdot\hat{x}$, as shown in Fig. S7. For example, the tangential field induced by an "up" dimer is

$$E_{t,\mathrm{up}} \sim -\frac{V_p}{2H}e^{-j\omega t}\frac{\alpha^2-j\alpha}{1+\alpha^2}\left[\left(K_1'+jK_1''\right)f_1(r)+\left(K_2'+jK_2''\right)g_2(r)\right] \tag{S8}$$

and the tangential field induced by a "down" dimer is

$$E_{t,\mathrm{down}} \sim -\frac{V_p}{2H}e^{-j\omega t}\frac{\alpha^2-j\alpha}{1+\alpha^2}\left[\left(K_2'+jK_2''\right)f_2(r)+\left(K_1'+jK_1''\right)g_1(r)\right] \tag{S9}$$

In both equations, $f_i(r)$ and $g_i(r)$ dictate the r-dependence of the tangential field:

$$f_1(r)=\frac{3\left(r/R_1\right)}{\left[1+\left(r/R_1\right)^2\right]^{5/2}} \qquad f_1(r)=\frac{3\left(r/R_2\right)}{\left[1+\left(r/R_2\right)^2\right]^{5/2}} \tag{S10}$$

$$g_1=\frac{3\left(2R_2/R_1+1\right)\left(r/R_1\right)}{\left[\left(2R_2/R_1+1\right)^2+\left(r/R_1\right)^2\right]^{5/2}} \qquad g_2=\frac{3\left(2R_1/R_2+1\right)\left(r/R_2\right)}{\left[\left(2R_1/R_2+1\right)^2+\left(r/R_2\right)^2\right]^{5/2}} \tag{S11}$$

Following Eq. (S7), it can be shown that the EHD velocity initiated by an "up" dimer is

$$u_{EHD}^{up} \sim \frac{\mathrm{C}}{2\mu}\left[\mathrm{K}_1''f_1(r)+K_2''g_2(r)\right] \tag{S12}$$

while EHD velocity initiated by a "down" dimer is

$$u_{EHD}^{down} \sim \frac{\mathrm{C}}{2\mu}\left[\mathrm{K}_2''f_2(r)+K_1''g_1(r)\right] \tag{S13}$$

Not surprisingly, the EHD velocities depend on the imaginary part of the polarizability coefficients of both lobes, with different r-dependent terms included to account for the influences of both top and bottom lobes.

2.3 The EHD interaction for standing dimers

Once we obtain the EHD velocity $u_{EHD}(r)$, we can calculate the EHD interactions by

$$\phi_{EHD}(r) = \int_{r}^{\infty} 6\pi\mu u_{EHD}(r) af(e) dr' \tag{S14}$$

where $f(e)$ is a function of the eccentricity.[8] For a sphere, $e = 0$ and $f(e) = 1$. Substituting Eq. (S7) into Eq. (S14), we obtain the EHD interaction between two spheres

$$\phi_{EHD}(r) \sim \frac{3\pi CK''\mathrm{R}^2}{\left[1+(r/R)^2\right]^{3/2}} \tag{S15}$$

Similarly, the EHD interaction between two "up" dimers is

$$\phi_{EHD}^{up}(r) \sim 3\pi \mathrm{C} af(e) \left\{ \frac{\mathrm{K}_1'' R_1}{\left[1+(r/R_1)^2\right]^{3/2}} + \frac{K_2'' R_2 (2R_1/R_2+1)}{\left[(2R_1/R_2+1)^2+(r/R_2)^2\right]^{3/2}} \right\} \tag{S16}$$

and the EHD interaction between two "down" dimers is

$$\phi_{EHD}^{down}(r) \sim 3\pi \mathrm{C} af(e) \left\{ \frac{\mathrm{K}_2'' R_2}{\left[1+(r/R_2)^2\right]^{3/2}} + \frac{K_1'' \mathrm{R}_1 (2R_2/R_1+1)}{\left[(2R_2/R_1+1)^2+(r/R_1)^2\right]^{3/2}} \right\} \tag{S17}$$

References

1. Nadal F, Argoul F, Hanusse P, Pouligny B, Ajdari A. Electrically induced interactions between colloidal particles in the vicinity of a conducting plane. *Physical Review E* **65**, 061409 (2002).

2. Dutcher CS, Woehl TJ, Talken NH, Ristenpart WD. Hexatic-to-Disorder Transition in Colloidal Crystals Near Electrodes: Rapid Annealing of Polycrystalline Domains. *Phys Rev Lett* **111**, 128302 (2013).

3. Ristenpart WD, Aksay IA, Saville DA. Assembly of colloidal aggregates by electrohydrodynamic flow: Kinetic experiments and scaling analysis. *Phys Rev E* **69**, 021405 (2004).

4. Ristenpart WD, Aksay IA, Saville DA. Electrohydrodynamic flow around a colloidal particle near an electrode with an oscillating potential. *J Fluid Mech* **575**, 83-109 (2007).

5. Hollingsworth AD, Saville DA. A broad frequency range dielectric spectrometer for colloidal suspensions: cell design, calibration, and validation. *J Colloid Interf Sci* **257**, 65-76 (2003).

6. Jones TB. *Electromechanics of Particles*. Cambridge University Press (1995).

7. Zhou H, Preston MA, Tilton RD, White LR. Calculation of the electric polarizability of a charged spherical dielectric particle by the theory of colloidal electrokinetics. *J Colloid Interf Sci* **285**, 845-856 (2005).

8. Chwang AT, Wu TY. Hydromechanics of low-Reynolds-number flow. Part 4. Translation of spheroids. *J Fluid Mech* **75**, 677-689 (1976).